ACADEMIC PRESS

Available online at www.sciencedirect.com

SCIENCE DIRECT®

Journal of Solid State Chemistry 175 (2003) 245–251

JOURNAL OF SOLID STATE CHEMISTRY

http://elsevier.com/locate/jssc

Hydrothermal homogeneous urea precipitation of hexagonal $YBO_3:Eu^{3+}$ nanocrystals with improved luminescent properties

Xiao-Cheng Jiang, Chun-Hua Yan,* Ling-Dong Sun,* Zheng-Gui Wei, and Chun-Sheng Liao

State Key Laboratory of Rare Earth Materials Chemistry and Applications, PKU-HKU Joint Laboratory on Rare Earth Materials and Bioinorganic Chemistry, College of Chemistry and Molecular Engineering, Peking University, Beijing 100871, China

Received 1 March 2003; received in revised form 1 May 2003; accepted 6 May 2003

Abstract

Well-crystallized $YBO_3:Eu^{3+}$ nanocrystals were prepared by a mild hydrothermal method in the presence of urea, and a pure hexagonal phase could be obtained at a low temperature of 200°C only. The photoluminescence spectra showed a remarkable improvement on the chromaticity as well as the luminescent intensity, compared with the samples synthesized by solid-state reaction (SR). The effects of the synthesis temperature, urea concentration, and the doping concentration of Eu^{3+} on the crystallization and luminescent properties were investigated. The results showed that both high temperature and low urea concentration were favorable to the formation of $YBO_3:Eu^{3+}$, and the ratio of red emission ($^5D_0 \rightarrow {}^7F_2$) to orange emission ($^5D_0 \rightarrow {}^7F_1$) increased with decreasing the synthesis temperature and the urea concentration. Furthermore, the samples exhibited a higher quenching concentration of Eu^{3+} in comparison with those prepared by the SR, which was beneficial to further enhancing the luminescent intensity. These synthesis-dependent phenomena were analyzed, and possible explanations were proposed.
© 2003 Elsevier Inc. All rights reserved.

Keywords: Nanocrystals; Phosphors; Hydrothermal; Chromaticity; Luminescence; Quenching

1. Introduction

Over the last few years, much attention has been paid to the synthesis and luminescent properties of Eu^{3+}-doped rare-earth orthoborates ($REBO_3$) due to their desirable properties as ideal vacuum ultraviolet phosphors, whose progress is key to the development of plasma display panels (PDPs) [1]. Various synthesis techniques have been developed to prepare high-quality $REBO_3:Eu^{3+}$ phosphors, such as solid-state reaction (SR) [1,2], coprecipitation [3,4], microwave heating [5], spray pyrolysis [6], and sol–gel method [4], but most of them only aimed at the enhancement of photoluminescence. For PDP phosphors, both luminescent efficiency and color purity are required. Unfortunately, as a red phosphor, the intensity of red emission of $REBO_3:Eu^{3+}$ is lower than that of the orange one, leading to a poor chromaticity.

Since the red emission, which comes from $^5D_0 \rightarrow {}^7F_2$ transition, is hypersensitive to the symmetry of the crystal field around Eu^{3+} and will be relatively strong if the symmetry of the crystal field is low, we attempted to reduce the symmetry of the crystal field to solve the chromaticity drawback of $YBO_3:Eu^{3+}$, in terms of increasing the contribution of $^5D_0 \rightarrow {}^7F_2$ transition. The synthesis of nanosized $YBO_3:Eu^{3+}$ was a possible solution because of the high disorder near its surface, and we achieved this approach by thermal decomposition of precursors that contained *RE*–EDTA and H_3BO_3–EDTA complexes [7–9]. Due to the lower site symmetry of Eu^{3+} in smaller-sized samples, the ratio of red emission to orange emission increased, leading to a better chromaticity. However, because of the existence of residual unburnt organic impurities as well as the uncompleted crystallization at lower temperatures ($\leqslant 700$°C), as-prepared samples exhibited a much lower luminescent intensity in comparison with the sample prepared by SR. Moreover, since the whole process, which involved an uncompleted burning step before pyrolysis, was pollution causing and not controllable, it may still have a long way to go for practical uses.

Our present work is aiming at developing a mild, clean, and controllable method to prepare $YBO_3:Eu^{3+}$

*Corresponding authors. Fax: +86-10-62754179.
E-mail address: chyan@chem.pku.edu.cn (C.-H. Yan).

0022-4596/03/$ - see front matter © 2003 Elsevier Inc. All rights reserved.
doi:10.1016/S0022-4596(03)00276-7

nanocrystals with better chromaticity and high luminescent efficiency. Hydrothermal technique is a good choice due to its convenience, exemption from pollution, and the possibility of achieving satisfying crystallinity at a relatively low temperature, without further calcination. Recently, Wang et al. [10] successfully synthesized non-aggregated $GdBO_3$:Eu^{3+} particles by a hydrothermal method, starting from the residual mixture that obtained by evaporating the solution of $Gd(NO_3)_3$, $Eu(NO_3)_3$, and H_3BO_3. An enhanced photoluminescence was observed, but since a high temperature of 300°C was required to gain a pure hexagonal phase in such a direct hydrothermal method, only submicron-sized particles could be produced, and there was little improvement on color purity. In order to prepare nano-sized YBO_3:Eu^{3+} phosphor in milder conditions in which Eu^{3+} ions would possess sites with lower symmetry and ameliorate the chromaticity, we chose the method of hydrothermal homogeneous urea precipitation, i.e., homogeneous precipitation of YBO_3:Eu^{3+} in a hydrothermal system in the presence of urea. This is a method that has been widely used for the synthesis of nanomaterials with superior homogeneity and particle size uniformity [11–14], and will help to achieve our aforementioned goals.

2. Experimental

YBO_3:Eu^{3+} nanocrystals were prepared from boric acid, urea, Y_2O_3, and Eu_2O_3. Appropriate amounts of Y_2O_3, Eu_2O_3, and H_3BO_3 were dissolved in dilute HNO_3, with the total concentration of metal cation being 0.05 mol/L. The initial pH value was controlled to be 4, and by the addition of a given amount of urea with concentrations ranging from 0.025 to 0.10 mol/L, a series of stock solutions could be prepared. A given volume (85 mL) of the stock solution was poured into a Teflon bottle (100 mL) held in a stainless-steel autoclave. After the autoclave was sealed tightly, it was placed in a temperature-controlled electric oven, heated at 80°C for 24 h, and subsequently heated at temperatures of 180–260°C for 12–48 h. The precipitated powders were separated by centrifugation, washed with deionized water and ethanol for several times, then dried in a vacuum oven at about 80°C for 12 h. For comparison, bulk YBO_3:Eu^{3+} was obtained by a direct SR from the mixture of Y_2O_3, Eu_2O_3, and H_3BO_3 at 1100°C for 10 h in air.

X-ray diffraction (XRD) studies were carried out on a Rigaku D/max-2000 X-ray powder diffractometer using CuKα ($\lambda = 1.5408$ Å) radiation. Transmission electronic microscopy (TEM) images were taken on a Hitachi H-8000 NAR TEM under a working voltage of 300 kV. An inductively coupled plasma atomic emission spectroscopy (ICP-AES, Plasma-Spec, Leeman Labs. Inc.) was used to analyze the chemical composition of the final products. Fluorescence spectra were recorded on a Hitachi F-4500 spectrophotometer equipped with a 150 W Xe-arc lamp at room temperature, and for comparison of different samples, the emission spectra were measured at a fixed band pass of 0.5 nm with the same instrument parameters.

3. Results and discussion

Fig. 1 showed the XRD patterns of $Y_{0.9}BO_3$:$Eu_{0.1}$ prepared with the same urea concentration of 0.025 mol/L under different temperatures of 180°C, 200°C, 220°C, 240°C, and 260°C for 24 h, which could be denoted as a1, b1, c1, d1, and e1, respectively. The XRD pattern of SR was also presented. When the sample was prepared under 180°C, product (a1) was mainly composed of $RE(OH)CO_3$. By increasing temperature, $RE(OH)CO_3$ could be changed into the target product, orthoborate, and a pure hexagonal phase of YBO_3:Eu^{3+} was obtained at 200°C. However, compared with the XRD pattern of SR, the relative intensities of different peaks changed greatly with synthesis temperature for as-prepared samples. The intensity ratio of (002) to (100), as well as that of (004) to (110) increased with the preparation temperature. The XRD pattern of e1, the sample prepared under the highest temperature (260°C), was in accordance with Wang's work [10]. Wang et al. attributed the abnormality from the JCPDS card (16–0277) to the hydrothermal process itself, while we considered that it also came from their extremely high synthesis temperature (300°C) under hydrothermal conditions. Similar correlation between preparation temperature and relative intensities of XRD peaks was also observed by Kim et al. [3], but due to the lack of control in a traditional coprecipitation process, this phenomenon was not

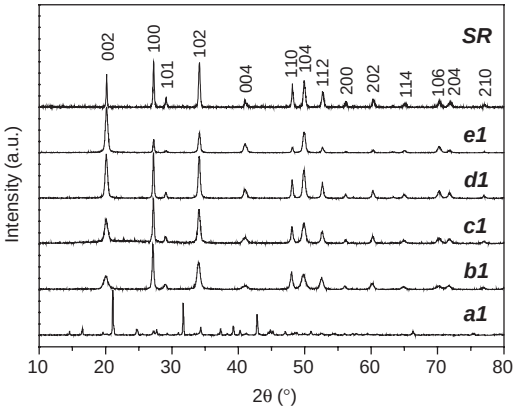

Fig. 1. XRD patterns of $Y_{0.9}BO_3$:$Eu_{0.1}$ prepared under different temperatures. The samples with the synthesis temperature of 180°C, 200°C, 220°C, 240°C, and 260°C were denoted as a1, b1, c1, d1, and e1, respectively. The sample fabricated by the solid-state reaction was denoted as SR. The denotation was same in following figures.

properly ascribed either. Besides the variance of relative intensities, the diffraction peaks also broadened with decreasing temperature, indicating smaller-sized particles could be obtained at a lower temperature, which coincided with the results from TEM images, as shown in Fig. 3.

Fig. 2 exhibited the influence of urea concentration on the XRD patterns. Nanocrystalline $Y_{0.9}BO_3$:$Eu_{0.1}$ synthesized under 240°C for 24 h with different urea concentrations of 0.025, 0.05, 0.075, and 0.100 mol/L were denoted as d1, d2, d3, and d4, respectively. The results showed that the concentration of urea also affected the preparation, and a high concentration of urea was not favorable to the formation of orthoborates. The XRD pattern of d4, prepared with the highest urea concentration, was similar to that of a1, and the peaks could be mainly indexed to $RE(OH)CO_3$. Like the impact of temperature on the XRD patterns, different urea concentration could also change the relative intensity of certain peaks greatly. The intensity ratio of (002) to (100), as well as that of (004) to (110), increased with decreasing the urea concentration. Combined with the information from Fig. 1, we could conclude that the transformation of XRD patterns may be attributed to the preferential nucleation and growth of crystals. This viewpoint is confirmed by the plate-like morphology of the final samples, as shown in Fig. 3, indicating that the preferential growth was along certain plane, resulting in larger plates with the growth of crystals. Any factors that could accelerate this process would cause the increase of the relative intensity of peak (002) and (004) due to the strengthened preferential orientation when performing XRD characterizations, such as a high temperature and a low urea concentration. Crystallization temperature was the key parameter controlling the strength of the interparticle bonds [15], and a higher temperature, which strengthened the interparticle bonds, favored the preferential nucleation.

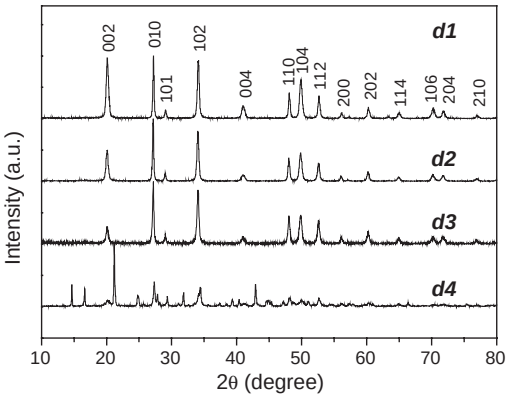

Fig. 2. XRD patterns of $Y_{0.9}BO_3$:$Eu_{0.1}$ prepared under 240°C with different urea concentrations of 0.025 (d1), 0.05 (d2), 0.075 (d3), and 0.100 mol/L (d4), respectively. The denotation was same in following figures.

A high urea concentration, however, would lead to a high level of CO_3^{2-} in the system. It could exist as a hindrance to the process by stabilizing certain surfaces that possess the high surface energy, thus weaken the selectivity of the growth. However, the line width showed no major difference for samples d1, d2, and d3, indicating the urea concentration had less impact on the size of YBO3:Eu^{3+} nanocrystals compared with the temperature.

Based on the XRD results, we deduced the whole reaction involved into two stages: (i) the formation of subcarbonate under hydrolysis of urea at lower temperatures and (ii) the reaction between subcarbonate and boric acid producing the final products under higher temperatures. In this work, a two-step process was adopted correspondingly in order to achieve the homogeneous precipitation of the phosphors, and the ratio of Y^{3+} to Eu^{3+} of the final products, as revealed by the ICP-AES results, was well accordant with the starting materials. For b1, for example, with 10 mol% Eu incorporated at first, the final concentration of Eu^{3+}, was determined as 9.9 at% after the two-step process. However, if the stock solution was directly subjected to the high-temperature hydrothermal process, the final composition would deviate from the initial one, with the concentration of Eu^{3+} to be 7.0 at%. This deviation could be attributed to the high rate of urea hydrolysis under harsh hydrothermal conditions, which would result in the inhomogeneity of the precipitation process.

Fig. 3 displayed the TEM images of samples prepared under different temperatures. All these samples exhibited a flake-like morphology, different from SR that possessed a sphere-like morphology with the particle size of about 1–2 μm. This two-dimensional growing habit coincided with the concept of preferential nucleation in this system. For b1, which was prepared under a low temperature of 200°C, there were only irregular small scraps with an average size of about 20 nm. When the temperature increased to 220°C, some scraps began to grow along certain plane to form larger ones of about 50 nm, with dissolving other small scraps simultaneously. Under 240°C, when the particle size continued to increase, a regular morphology of hexagonal flake was also observed, indicating that the crystals were better crystallized. And at the highest temperature of 260°C, hexagonal flakes with largest size of more than 100 nm and best crystallinity were produced. The whole process disclosed that a high temperature would lead to larger particle size and better crystallization, which was crucial to our comprehension of the luminescent properties of as-prepared samples.

The emission spectra of e1 and SR under 240 nm UV irradiation were shown in Fig. 4. Generally, the spectra of YBO_3:Eu^{3+} consist of sharp lines ranging from 580 to 720 nm, which are associated with the transitions from the excited $^5D_0$ level to ^7F_J ($J = 1$, 2, 3, and 4)

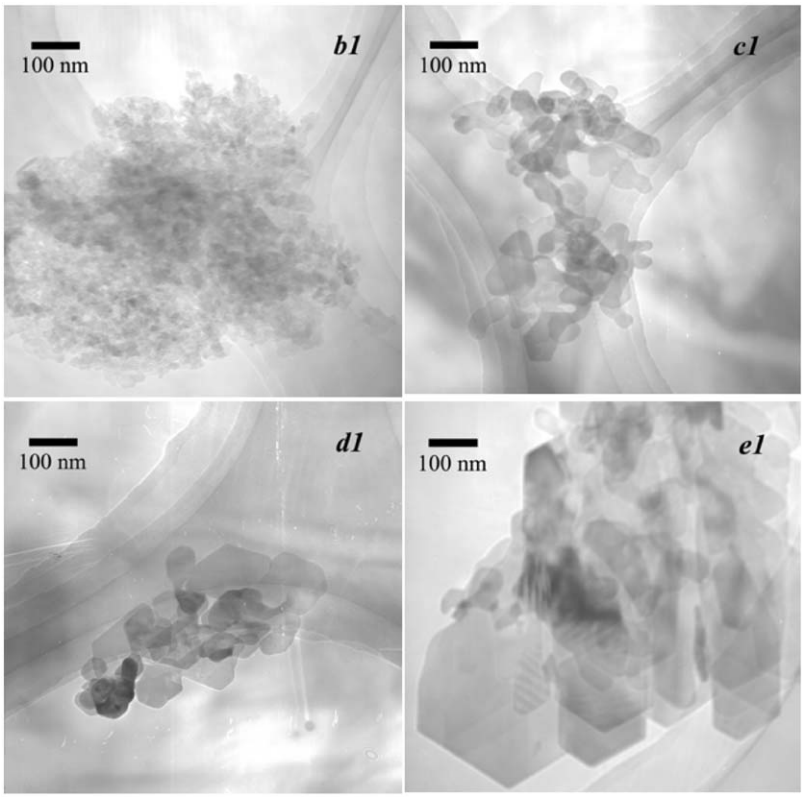

Fig. 3. TEM images of $Y_{0.9}BO_3$:$Eu_{0.1}$ for samples b1, c1, d1, and e1.

levels of Eu^{3+} activators [16,17]. As can be seen, for e1, the ratio of the red emission at 610 nm to the orange one at 591 nm (R/O value) was much higher than that of SR. This phenomenon could be explained by Judd–Ofelt theory [18]. The red emission at 610 nm from $^5D_0 \rightarrow {}^7F_2$ transition is a typical electric dipole transition, while the orange emission at 591 nm from $^5D_0 \rightarrow {}^7F_1$ transition is a typical magnetic dipole transition. The relative intensity of them depends strongly on the local symmetry of Eu^{3+} ions, and a lower symmetry of crystal field around Eu^{3+} ions will result in a higher R/O value. This low crystal field symmetry and the subsequent better chromaticity could be achieved in nanoparticles due to their high degree of disorder near the surface, as pointed out by many authors [19–24]. Besides the improvement on chromaticity, we could also observe an increase on the photoluminescent intensity of e1. Generally, nano-sized phosphors always exhibit lower luminescence efficiency. It is true for b1, c1, and d1. This lower luminescence efficiency may come from various pathways of non-radiative relaxation for nanomaterials. In aqueous solutions, as pointed out by Maas et al. [25], the existence of a small amount of OH^- coordinated to lanthanide ions at the surface should be responsible for the poor photoluminescence. For sample b1, c1 and d1, since the synthesis temperatures were relatively low, the $-$OH surface groups still exist and take the function as multiphonon relaxation centers. [26] As a result, the photoluminescence was lower than the sample SR, although the chromaticity was improved. A high-temperature hydrothermal treatment would help to eliminate both –OH groups and other defects. So as the temperature increased to 260°C, a higher luminescent intensity was achieved. At the same time, since no mechanical milling process, which would be harmful to the luminescent properties as pointed by Wang et al. [10], was included in this method, and better crystalline integrity was also achieved under hydrothermal

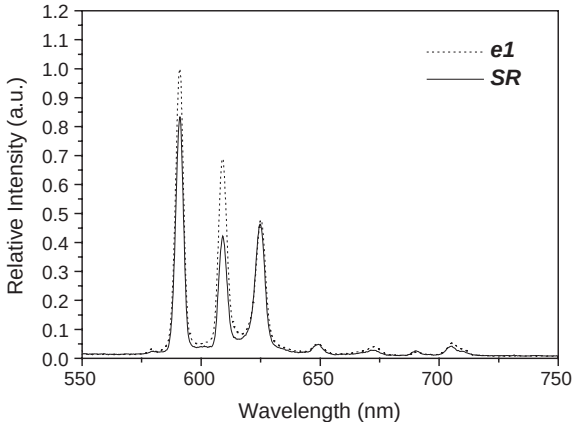

Fig. 4. Emission spectra of $Y_{0.9}BO_3$:$Eu_{0.1}$ for samples e1 and SR, under 240 nm UV irradiation.

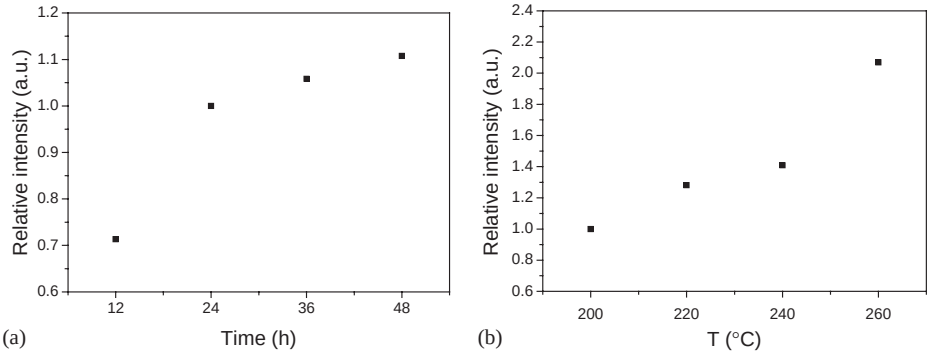

Fig. 5. Relative intensity of the emission at 591 nm to that of sample b1 (a) with different reaction time, whose synthesis temperature and urea concentration were controlled to be 200°C and 0.025 mol/L, respectively; (b) under different temperature, whose reaction time and urea concentration were controlled to be 24 h and 0.025 mol/L, respectively.

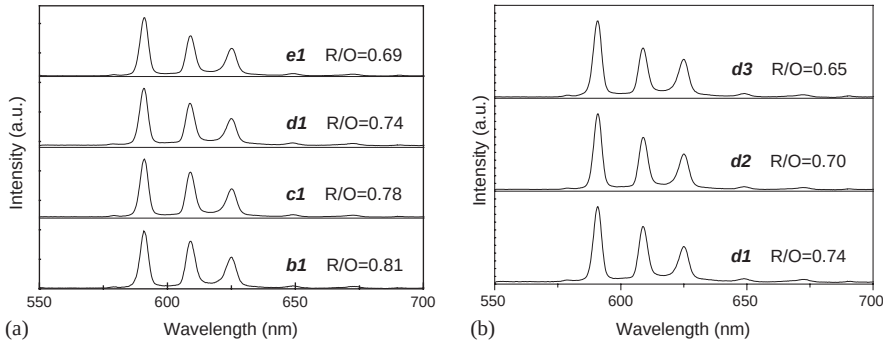

Fig. 6. Emission spectra of $Y_{0.9}BO_3:Eu_{0.1}$ under 240 nm irradiation for samples: (a) b1, c1, d1, and e1; (b) d1, d2, and d3. All of them were normalized with the peak at 591 nm.

conditions, the photoluminescence of e1 even exceeded that of SR, as can be seen from the spectra.

The changes of the relative intensity of the emission at 591 nm to that of b1 according to different synthesis temperature and time were shown in Fig. 5. Fig. 5(a) showed the influence of reaction time when all the other conditions were the same to b1, and we could find that a longer reaction time would result in a stronger emission, which may come from the better crystallinity caused by the longer crystallization time. Since when the time was over 24 h, the emission intensity changed more slowly, a reaction time of 24 h would be a reasonable choice. In Fig. 5(b), for b1, c1, d1, and e1, the emission intensity increased gradually with the temperature at first, and at 260°C, a more obvious increase was observed. Combined with above discussions, we consider that temperature affected the luminescent efficiency by improving the crystallinity and eliminating the −OH surface groups. At 260°C, as can be seen from both the XRD patterns and TEM images, best crystallinity was achieved, resulting in the highest luminescent intensity.

Fig. 6 displayed the emission spectra of $Y_{0.9}BO_3:Eu_{0.1}$ prepared at different temperatures and pH values under 240 nm UV radiation, all of which were normalized with the peak at 591 nm in order to compare the relative intensity between different peaks. In Fig. 6(a), we could clearly observe the temperature-dependent characteristic of R/O value. For b1, c1, d1, and e1, the R/O value was 0.81, 0.78, 0.74, and 0.69, respectively, indicating a lower temperature was favorable to achieve superior chromaticity. The temperature affected the R/O value by controlling the particle size and crystallization, both of which had a great impact on the chromaticity. Our previous work has demonstrated that the sites at the surface in $YBO_3:Eu^{3+}$ nanocrystals were of lower site symmetry, thus inducing a higher R/O value, while interior sites were of high site symmetry and caused a lower one [8]. When the particle size increased with the increase of temperature, as was shown in TEM graphs, the number of surface sites was reduced, resulting in poorer color purity. At the same time, the particles were better crystallized, which would cause a lower level of disorder [27,28], further lowering the R/O value. Similarly, in Fig. 6(b), we could also observe an obvious change of chromaticity. For a larger urea concentration, the phosphor exhibited a lower R/O value. In this case, we could deduce that this decrease of R/O value might come from some factor other than the change of particle size, since the particle size showed no major difference with changing the urea concentration. Sheng et al. [29] once reported the variation of relative luminescent intensity of two sites with different symmetry caused

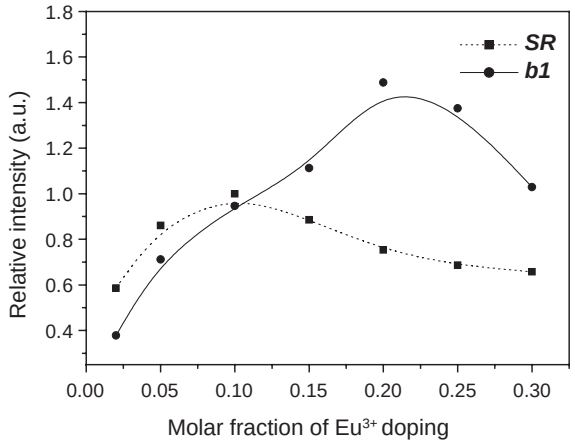

Fig. 7. Quenching concentration of $Y_{1-x}BO_3:Eu_x$ for samples b1 and SR obtained by monitoring the emissions of $^5D_0$–$^7F_2$ at 610 nm.

by a preferential chemical attack of H_2O on certain site, and in our case, it may come from the selective attack of OH^-. Since the sites correlated with the red emission are of a lower symmetry and reside at the surface, they face higher probability of being quenched by OH^- compared with those in the interior. With the increase of the urea concentration, the intensity of the red emission declined faster than that of the orange one, resulting in a lower R/O value.

The relationship between luminescence intensity by monitoring the emissions of $^5D_0$–$^7F_2$ at 610 nm and Eu^{3+} dopant content for samples b1 and SR was shown in Fig. 7. The quenching concentration was about 10% for bulk $YBO_3:Eu^{3+}$, and increased to 22% for sample b1, whose particle size was about 20 nm. Generally, the concentration quenching effect is ascribed to the possible non-radiative transfer between neighboring Eu^{3+} ions, which increases the mobility of the excited state within the host matrix and therefore increases the probability of non-radiative de-excitation via traps [30,31]. In nanomaterials, the limited primitive cells per particle results in the fact that the traps distribute randomly with a considerable fluctuation between particles [30]. Since resonance energy transfer only occurs within one particle due to the hindrance by the particle boundary, when increasing the concentration of luminescent centers, quenching occurs first in particles containing many traps, while those particles containing few or no traps quench only at high concentration or do not quench at all. Therefore, quenching occurs at higher Eu concentration in smaller particles. Such a desirable characteristic of $YBO_3:Eu^{3+}$ nanocrystals could overcome their disadvantages of the lower luminescent efficiency compared with bulk $YBO_3:Eu^{3+}$, especially when the particle size was too small, by doping more Eu^{3+} into the host materials, and was of great benefit to their practical uses.

4. Conclusion

In this work, a clean and convenient method, the hydrothermal homogeneous urea precipitation, was introduced to synthesize high-quality $YBO_3:Eu^{3+}$ phosphor under mild conditions. As-prepared phosphor showed many desirable characteristics, such as high luminescent efficiency, improved chromaticity, and a higher quenching concentration of Eu^{3+}. The effects of synthesis temperature and urea concentration on the phase formation and luminescent properties were studied, showing that both the luminescent intensity and color purity were correlated with the reaction conditions. Low temperature of preparation favors smaller particles with lower luminescent intensity but better chromaticity, while high temperature will lead to higher luminescent intensity. This disadvantage can be overcome using a higher concentration of Eu^{3+} dopants due to the increase of the quenching concentration, thus resulting in phosphors with best qualities.

Acknowledgments

This work is supported by the NSFC (20001002, 20013005, and 20221101), MOST (G19980613), MOE (the Foundation for University Key Teacher), the Founder Foundation of PKU, and Hui-Chun Chin and Tsung-Dao Lee Chinese Undergraduate Research Endowment (CURE).

References

[1] M. Ren, J.H. Lin, Y. Dong, L.Q. Yang, M.Z. Su, L.P. You, Chem. Mater. 11 (1999) 1576.
[2] X.Y. Wu, G.Y. Hong, X.Q. Zeng, H.P. You, C.H. Kim, C.H. Pyun, H.S. Bal, B.Y. Yu, I.E. Kwon, C.H. Park, Chem. J. Chin. U. 21 (2000) 1658.
[3] K.N. Kim, H.K. Jung, H.D. Park, D. Kim, J. Mater. Res. 17 (2002) 907.
[4] D. Boyer, G. Bertrand-Chadeyron, R. Mahiou, C. Caperaa, J.C. Cousseins, J. Mater. Chem. 9 (1999) 211.
[5] Y.Y. Li, M.L. Peng, S.H. Feng, Chin. Chem. Lett. 7 (1996) 387.
[6] D.S. Kim, R.Y. Lee, J. Mater. Sci. 35 (2000) 4777.
[7] Z.G. Wei, L.D. Sun, C.S. Liao, C.H. Yan, Appl. Phys. Lett. 80 (2002) 1447.
[8] Z.G. Wei, L.D. Sun, C.S. Liao, J.L. Yin, X.C. Jiang, C.H. Yan, J. Phys. Chem. B 106 (2002) 10610.
[9] Z.G. Wei, L.D. Sun, C.S. Liao, X.C. Jiang, C.H. Yan, J. Mater. Chem. 12 (2002) 3665.
[10] Y.H. Wang, K. Uheda, H. Takizawa, T. Endo, Chem. Lett. 3 (2001) 206.
[11] S. Somiya, T. Akiba, Z. Nakai, K. Hishinuma, T. Kumaki, Y. Suwa, J. Aust. Ceram. Soc. 26 (1990) 171.
[12] M. Hirano, M. Inagaki, J. Mater. Chem. 10 (2000) 473.
[13] D. Mishra, S. Anand, R.K. Panda, R.P. Das, J. Am. Ceram. Soc. 85 (2002) 437.
[14] M. Hirano, N. Sakaida, J. Ceram. Soc. Jpn. 111 (2003) 176.

[15] J. Tartaj, E. Lachowski, J.F. Fernandez, C. Moure, P. Duran, J. Eur. Ceram. Soc. 20 (2000) 169.
[16] R.T. Wegh, H. Donker, K.D. Oskam, A. Meijerink, Science 283 (1999) 663.
[17] C. Feldmann, T. Jüstel, C.R. Ronda, D.U. Wiechert, J. Lumin. 92 (2001) 245.
[18] B.R. Judd, Phys. Rev. 127 (1962) 750.
[19] Y. Tao, G.W. Zhao, W.P. Zhang, S.D. Xia, Mater. Res. Bull. 32 (1997) 501.
[20] Q. Li, L. Gao, D.S. Yan, Chem. Mater. 11 (1999) 533.
[21] D.K. Williams, B. Bihari, B.M. Tissue, J.M. McHale, J. Phys. Chem. B 102 (1998) 916.
[22] B.M. Tissue, Chem. Mater. 10 (1998) 2837.
[23] B.M. Tissue, B. Bihari, J. Fluoresc. 8 (1998) 289.
[24] H. Eliers, B.M. Tissue, Chem. Phys. Lett. 251 (1996) 74.
[25] H. Maas, A. Currao, G. Calzaferri, Angew. Chem. Int. Ed. 41 (2002) 2495.
[26] A. Huignard, T. Gacoin, J. Boilot, Chem. Mater. 12 (2000) 1090.
[27] Z.M. Qi, C.S. Shi, Y.G. Wei, Z. Wang, T. Liu, T.D. Hu, Z.Y. Zhao, F.L. Li, J. Phys.: Condens. Matter 13 (2001) 11503.
[28] Z.M. Qi, C.S. Shi, Z. Wang, Y.G. Wei, Y.N. Xie, T.D. Hu, F.L. Li, Acta Phys. Sin. 50 (2001) 1318.
[29] K.C. Sheng, G.M. Korenowski, J. Phys. Chem. 92 (1988) 50.
[30] W.P. Zhang, P.B. Xie, C.K. Duan, K. Yan, M. Yin, L.R. Lou, S.D. Xia, J.C. Krupa, Chem. Phys. Lett. 292 (1998) 133.
[31] J. Dhanaraj, R. Jagannathan, T.R.N. Kutty, C.H. Lu, J. Phys. Chem. B 105 (2001) 11098.